

Dynamic Restructuring Induced Oxygen Activation on AgCu Near-Surface Alloys

Laura A. Cramer,[§] Yilang Liu,[§] Prashant Deshlahra,* and E. Charles H. Sykes*



Cite This: *J. Phys. Chem. Lett.* 2020, 11, 5844–5848



Read Online

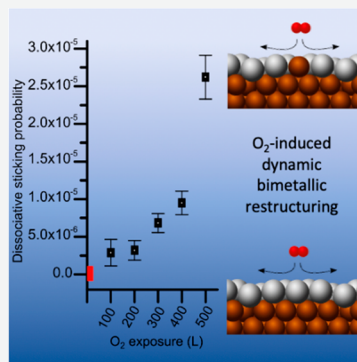
ACCESS |

Metrics & More

Article Recommendations

Supporting Information

ABSTRACT: Recent studies have shown that the addition of Cu to Ag catalysts improves their epoxidation performance by increasing the overall selectivity of the bimetallic catalyst. We have prepared AgCu near-surface alloys and used scanning tunneling microscopy to gain an atomistic picture of O₂ dissociation on the bimetallic system. These data reveal a higher dissociative sticking probability for O₂ on AgCu than on Ag(111), and density functional theory (DFT) confirms that the O₂ dissociation barrier is 0.17 eV lower on the alloy. Surprisingly, we find that, after a slow initial uptake of O₂, the sticking probability increases exponentially. Further DFT calculations indicate that surface oxygen reverses the segregation energy for AgCu, stabilizing Cu atoms in the Ag layer. These single Cu atoms in the Ag surface are found to significantly lower the O₂ dissociation barrier. Together, these results explain nonlinear effects in the activation of O₂ on this catalytically relevant surface alloy.



Selective oxidation reactions over heterogeneous catalysts produce key chemical intermediates such as aldehydes, ketones, epoxides, and organic acids that are used in the synthesis of many value-added products. The partial oxidation of ethylene to produce the important chemical precursor ethylene oxide is one of the most industrially relevant of these selective oxidations with a global production of 34.5 million tons in 2016.^{1–3} Great interest lies in understanding and optimizing this reaction as slight improvements in catalyst selectivity and activity can translate to large energy and cost savings. This reaction is typically performed on Ag-based catalysts where selectivity toward ethylene oxide can reach 80–90% through the use of promoters such as Cl and Cs.^{4–9} Though the catalysts can achieve high selectivity, they operate at around 15% conversion.¹⁰ O₂ activation plays an important role in this reaction, and atomic oxygen has been confirmed as the active species in both the partial and total oxidation pathways.¹¹ It has also been shown that selectivity toward ethylene oxide increases with increasing oxygen coverage.¹⁰ As such, much interest lies in the generation of these active oxygen species on relatively inert Ag(111).

Bimetallic alloys are a proven method to improve the overall efficiency of a given reaction while maintaining selectivity toward the desired product. The addition of Cu to heterogeneous Ag catalysts has been shown to improve epoxidation performance.^{12,13} While Cu has been demonstrated to improve the overall selectivity of the catalyst, its exact role is unknown.^{1,2} In this study, we explored the possibility of increasing the ability of Ag to activate O₂ by creating a near-surface alloy (NSA) consisting of a single atomic layer of Ag on Cu(111). NSAs consist of a solute metal

present in a lower concentration than the host metal and confined to the top, or, in some cases, to the subsurface layer of the alloy. The presence of a solute metal in the near-surface region alters the electronic and thus the catalytic properties of the alloy.^{14,15} Some NSAs possess desirable catalytic properties compared to the constituent metal counterparts as shown both in practice and in theory.^{15–20}

In a pioneering example, Greeley and Mavrikakis systematically calculated the reactivity toward hydrogen dissociation of NSAs consisting of one monolayer solute metal on the surface of a host metal or confined to the second (subsurface) layer.²¹ Their findings presented exciting new possibilities for hydrogenation catalysts. In practice, some of these NSAs have proven to behave differently in experiments than predicted by DFT, often reconstructing to reduce overall free energy of the system. One such case is Ag on Cu(111), which reconstructs to form a well-characterized 9 × 9 reconstruction in the underlying Cu(111) leading to a triangular pattern in the Ag layer. While the structure of this system is well-characterized, to the best of our knowledge its chemical reactivity has not been investigated.^{14,22–25}

Here, we report the first systematic study of molecular O₂ dissociation on the 9 × 9 AgCu NSA using STM and DFT and compare and contrast these results to the dissociation of O₂ on

Received: March 20, 2020

Accepted: June 30, 2020

Published: June 30, 2020



ACS Publications

© 2020 American Chemical Society

5844

<https://dx.doi.org/10.1021/acs.jpclett.0c00887>
J. Phys. Chem. Lett. 2020, 11, 5844–5848

Ag(111) under ultrahigh vacuum (UHV) conditions. Taken together, these experiments provide new insights into O₂ dissociation, spillover, and reaction at catalytically relevant Ag–Cu interfaces. Importantly, our statistical analysis of these experimental STM images shows that the dissociative sticking probability of O₂ on the AgCu NSA can be up to $\sim 2 \times 10^{-5}$, which is much higher than the literature value of $\sim 1.1 \times 10^{-7}$ for Ag(111).²⁶

We first examined the growth of Ag on Cu(111) at room temperature using STM and observed the characteristic 9 × 9 reconstruction (Figure 1a,b). Bellisario et al. have shown that,

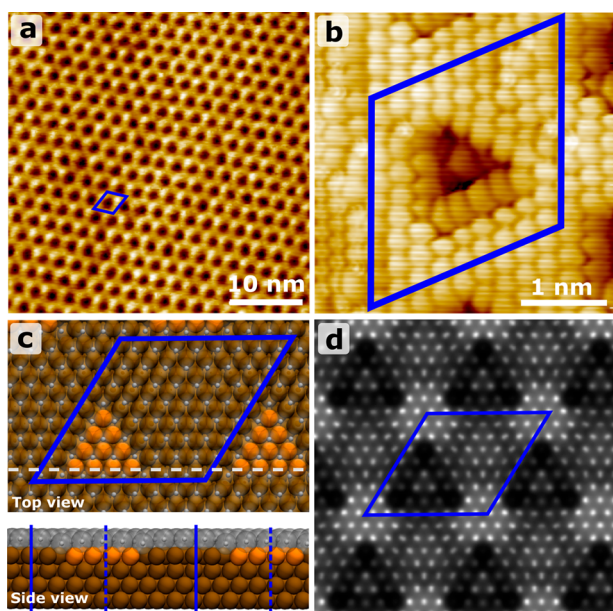


Figure 1. Visualizing the AgCu NSA. (a) Large scale STM image of AgCu NSA. Scanning conditions: 120 mV 15 pA. (b) Atomic resolution STM image of the AgCu NSA. Scanning conditions: 1V 55 nA. (c) Top and side view of the optimized DFT model. Ag atoms are shown as semitransparent silver spheres with dark silver dots at the center. Orange spheres represent atoms shifted to hcp positions in the top Cu layer. Brown spheres represent all other unperturbed Cu atoms. Blue parallelograms represent the 9 × 9 unit cell of the NSA. (d) DFT-simulated STM image.

upon deposition of Ag on Cu(111) at room temperature, Ag atoms traverse large distances (>100 nm) until encountering a step edge where the 2D 9 × 9 reconstructed Ag layer grows outward from the step.²⁷ Ag layer growth continues until a full monolayer is formed, at which point multilayer growth begins. The AgCu NSA reconstructs to relieve lattice strain due to the relatively large lattice mismatch of 13% between Ag and Cu (bulk $d_{\text{Ag}} = 0.289$ nm, bulk $d_{\text{Cu}} = 0.256$ nm). This reconstruction forms in the topmost Cu layer underneath the Ag monolayer via ejection of Cu atoms and the shift of approximately 20% of the underlying Cu atoms from fcc to hcp sites. This leads to a triangular dislocation loop and 9 × 9 reconstruction in the Cu that appears in STM images as a triangular pattern in the top Ag layer.¹⁶ The atomically resolved STM image of the AgCu NSA in Figure 1b shows a full unit cell with one of the repeating triangles. Figure 1c shows a DFT-optimized model of the atomic structure of this dislocation loop with first layer Cu atoms shifted from fcc to hcp sites represented as orange spheres and the remaining fcc Cu atoms as darker brown spheres while the small silver spheres represent the center of Ag atoms in the overlayer. A DFT-simulated STM image in Figure 1d shows the same repeating triangular pattern as that observed in the experimental STM images. To avoid confusion between the 9 × 9 reconstruction and the atomic resolution of the Ag overlayer which have a similar appearance, the blue parallelograms in Figure 1 indicate the 9 × 9 unit cell in each panel.

STM imaging after exposure of the AgCu NSA to molecular O₂ at 300 K revealed depressions within the 9 × 9 reconstruction that increased in number with increasing O₂ exposure (Figure 2a–f). These new features are distinguishable from the 9 × 9 reconstruction as randomly located depressions ~ 20 pm lower than the top Ag layer. Given that molecular O₂ desorbs from Ag below room temperature,²⁶ these depressions must be due to atomic O-adatoms resulting from molecular dissociation. Oxygen is known to image as a depression in STM, in line with our assignment of the features as O-adatoms.^{28–30} Furthermore, our DFT-simulated STM images of the bare AgCu NSA and the AgCu NSA with O-adatoms are consistent with the experimental imaging results (Figure S2a,b).

A statistical analysis was performed using multiple 50 nm × 50 nm STM images for each of the O₂ exposures in Figure 2a–

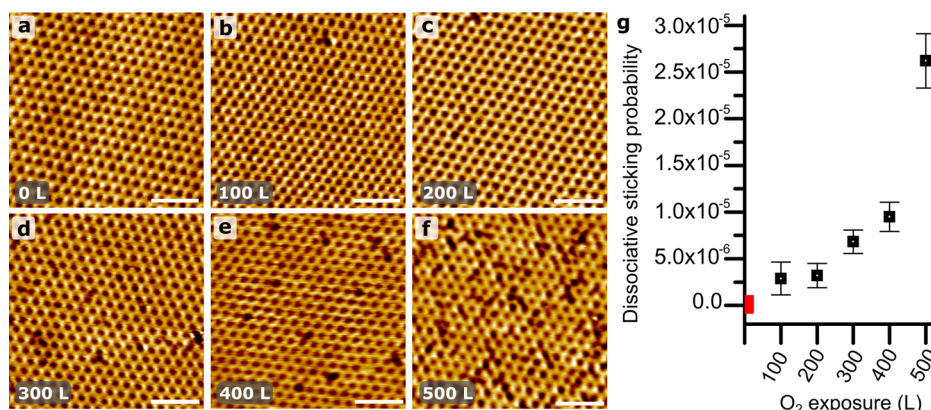


Figure 2. (a–f) Room temperature STM images of AgCu NSA with increasing exposure to O₂ at 300 K: (a) 0, (b) 100, (c) 200, (d) 300, (e) 400, and (f) 500 L (1 L = 1.0×10^{-6} Torr s). Scale bars are 10 nm. Imaging conditions: -120 mV, 15 pA. (g) Dissociative sticking probability of O₂ on AgCu NSA as a function of exposure to O₂ at 300 K. Error bars represent one standard deviation of the mean. Red square indicates initial dissociative sticking probability of 1.1×10^{-7} for O₂ on Ag(111) at 490 K under UHV conditions.²⁷

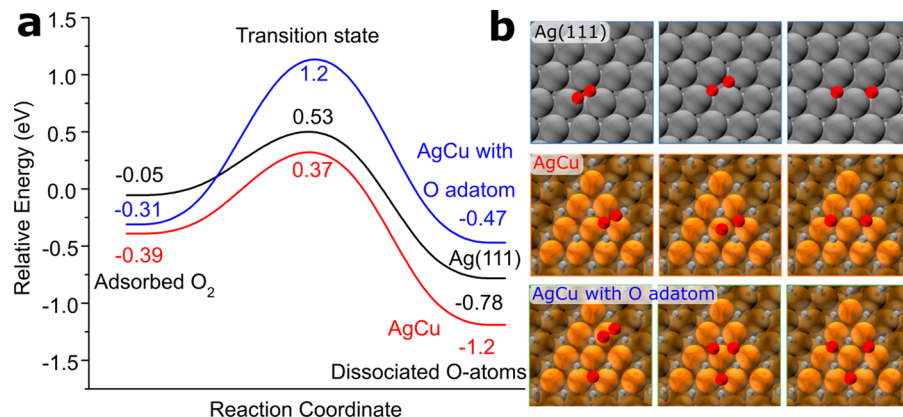


Figure 3. (a) Electronic energies as a function of reaction coordinate and (b) structures for O₂ dissociation on Ag(111) and AgCu showing an increased dissociation barrier in the presence of an O-adatom due to a repulsive interaction between adjacent O-adatoms. The O–O distances are shown in the Supporting Information (Table S3).

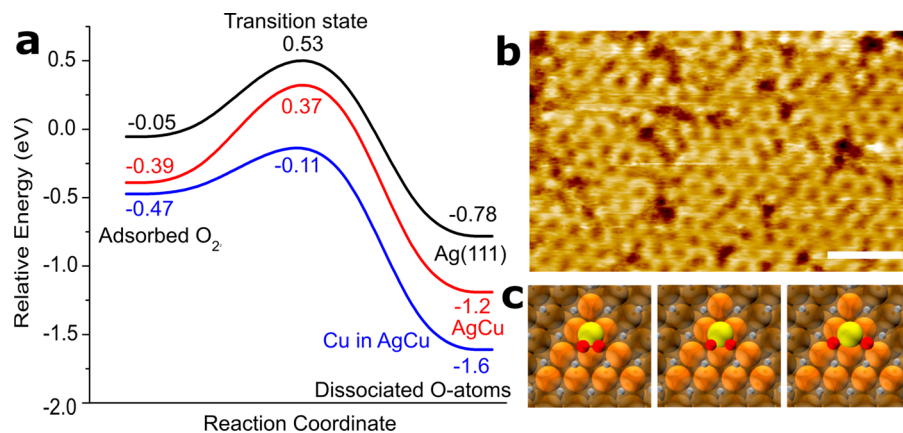


Figure 4. (a) Electronic energies as a function of reaction coordinate for O₂ dissociation on AgCu NSA showing a decreased dissociation barrier for a Cu atom in the Ag surface layer. (b) STM image of AgCu showing Cu_xO patches within the Ag layer. Scale bar is 10 nm. (c) Structure for O₂ dissociation on a Cu atom in the Ag layer of AgCu. Yellow and red spheres represent exposed Cu atoms and O-adatoms, respectively.

f. We were able to extract a dissociative sticking probability using this analysis, and the results are shown in Figure 2g. We found a sticking probability of 2.6×10^{-6} at the lowest O₂ exposure investigated (100 L O₂, Figure 2a). Interestingly, this is almost an order of magnitude higher than the reported sticking probability of O₂ on Ag(111) of $\sim 10^{-7}$.^{31,32} Furthermore, Figure 2g reveals that higher O₂ exposures lead to exponentially higher sticking probabilities reaching 2.6×10^{-5} for 500 L O₂. To avoid miscounting of small O-adatom clusters, each depression was conservatively counted as a single O-adatom meaning that the concentration of O-adatoms may in fact be higher than those quoted experimentally. Details of O-adatom analysis are included in Table S1 in the Supporting Information.

Previous studies of O₂ dissociation on Ag(111) under UHV conditions have shown that the O-adatom coverage increases linearly with increasing O₂ exposure.^{26,33} This is in sharp contrast to the nonlinear increase of O₂ dissociation probability with increasing O₂ exposure we see on the AgCu NSA. Though not common to Ag(111), this nonlinear increase is seen for O₂ dissociation on other metals. A temperature-programmed desorption (TPD) study of O₂ on Pt(111) attributed the increase in oxygen coverage with increasing exposure to O-adatom island formation.³⁴ Zambelli et al. studied this effect using STM and found that exposure of the

Pt(111) surface to 1 L of O₂ above 95 K led to O₂ dissociation with atomic O-adatoms clustering in 1D chains.³⁵ It was also found for Au(111) that the presence of O-adatoms increased the dissociation probability of O₂ by more than 3 orders of magnitude at 400 K and was also accompanied by O-adatom island formation.^{36,37}

We turned to DFT to investigate the origin of the increasing dissociative sticking probability with O₂ exposure in our AgCu NSA system. Figure 3 shows that the O₂ dissociation transition state energy relative to gas phase O₂ and bare surfaces is 0.53 eV on Ag(111) and 0.37 eV on the AgCu NSA. This is consistent with our STM derived initial sticking probability, which is much higher on AgCu than on Ag(111). Next, we examined the possibility of atomic O self-promoting further dissociation of molecular O₂ using DFT. Our results revealed a transition state energy of 1.2 eV for O₂ dissociation on AgCu near an O-adatom, following the pathway shown in Figure 3b. This arises from strong repulsive interactions between O-adatoms and O₂ molecules, ruling out the possibility of an autocatalytic process. Such repulsive interactions are in fact well-known to lead to a decreasing sticking probability with coverage, in sharp contrast to the exponential increase shown here.³⁸

We then considered the possibility of the AgCu NSA restructuring to expose a Cu active site for O₂ dissociation.

Such reverse-segregation of Cu is unfavorable in the bare NSA surface by +0.39 eV due to the higher surface free energy of Cu.³⁹ The strong O binding to the exposed Cu atom, however, compensates for the +0.39 eV restructuring energy of the bare NSA as shown by the adsorbed O₂ energy of −0.47 eV for the restructured NSA. Figure 4a shows the energy pathway for O₂ dissociation over an exposed Cu atom in the Ag layer after accounting for the restructuring energy (details in Supporting Information, Table S2). The transition state energy drops from 1.2 eV for the autocatalytic process just discussed to −0.11 eV for a single Cu atom in the Ag layer. This result is further supported by the appearance of Cu_xO patches within the Ag layer as seen in Figure 4b. For this process to occur, the surface segregation energy of Cu reverses and the AgCu NSA must undergo a dynamic restructuring to expose a Cu atom active site in the Ag layer. This finding is supported by previous studies that have shown the formation of Cu₂O on the surface of AgCu alloys under higher oxygen exposures.^{40,41} With this knowledge, we propose that there are two dissociation pathways that lead to the nonlinear increase in sticking probability plotted in Figure 2g. The first pathway is direct dissociation of O₂ on the perfect AgCu NSA at low exposures, and in another the Cu atoms are exposed within the Ag layer at higher O₂ exposures. The exponential increase in dissociative sticking probability arises from dissociated O-adatoms on the surface which make the exposure of more Cu atoms in the surface energetically favorable, which in turn lowers the barrier for subsequent O₂ dissociation. Details of the exponential relationship between dissociative oxygen uptake and oxygen exposure are provided in the Supporting Information under Section S6.

In summary, we have found that relatively low O₂ potentials are able to reverse the segregation energy for the AgCu NSA and dynamically restructure the NSA to expose Cu atoms in the surface layer. Higher O₂ pressures expose more Cu, which dramatically enhances the dissociative sticking probability. DFT reveals that a single Cu atom in the Ag layer can significantly reduce the O₂ activation barrier. Given that Ag is a ubiquitous element in selective oxidation catalysis in which selectivity often comes at the cost of conversion, this rate limiting O₂ activation step is important. It has been demonstrated that the addition of Cu to Ag promotes ethylene epoxidation, but its mode of action is currently unclear. Together, our results demonstrate how Cu, both in and under Ag, lowers O₂ activation barriers compared to pure Ag, which sheds some light on the role of even very dilute amounts of Cu in Cu-promoted Ag-based epoxidation reactions.^{12,13}

ASSOCIATED CONTENT

Supporting Information

The Supporting Information is available free of charge at <https://pubs.acs.org/doi/10.1021/acs.jpcllett.0c00887>.

STM and DFT methods, O-adatom coverages derived from STM images, simulated STM images, energy calculations accounting for NSA restructuring, and analysis of exponential O-adatom coverage increase (PDF)

AUTHOR INFORMATION

Corresponding Authors

Prashant Deshlahra — Department of Chemical and Biological Engineering, Tufts University, Medford, Massachusetts 02155,

United States;  orcid.org/0000-0002-1063-4379;

Email: Prashant.Deshlahra@tufts.edu

E. Charles H. Sykes — Department of Chemistry, Tufts University, Medford, Massachusetts 02155, United States;  orcid.org/0000-0002-0224-2084; Email: Charles.Sykes@tufts.edu

Authors

Laura A. Cramer — Department of Chemistry, Tufts University, Medford, Massachusetts 02155, United States

Yilang Liu — Department of Chemical and Biological Engineering, Tufts University, Medford, Massachusetts 02155, United States

Complete contact information is available at: <https://pubs.acs.org/10.1021/acs.jpcllett.0c00887>

Author Contributions

[§]L.A.C. and Y.L. contributed equally to this work.

Notes

The authors declare no competing financial interest.

ACKNOWLEDGMENTS

The experimental work was supported by the Division of Chemical Sciences, Office of Basic Energy Sciences, CPIMS Program, U.S. Department of Energy, under Grant DE-SC0004738. Y.L. and P.D. acknowledge support from the National Science Foundation (Award 1803798) and computational resources from XSEDE⁴² (Award ACI-1548562) for the theory work.

REFERENCES

- (1) Linic, S.; Jankowiak, J. T.; Barteau, M. A. Selectivity Driven Design of Bimetallic Ethylene Epoxidation Catalysts from First Principles. *J. Catal.* **2004**, *224* (2), 489–493.
- (2) Greiner, M. T.; Cao, J.; Jones, T. E.; Beeg, S.; Skorupska, K.; Carbonio, E. A.; Sezen, H.; Amati, M.; Gregoratti, L.; Willinger, M. G.; Knop-Gericke, A.; Schlägl, R. Phase Coexistence of Multiple Copper Oxides on AgCu Catalysts during Ethylene Epoxidation. *ACS Catal.* **2018**, *8* (3), 2286–2295.
- (3) Pu, T.; Tian, H.; Ford, M. E.; Rangarajan, S.; Wachs, I. E. Overview of Selective Oxidation of Ethylene to Ethylene Oxide by Ag Catalysts. *ACS Catal.* **2019**, *9*, 10727–10750.
- (4) Özbek, M. O.; Van Santen, R. A. The Mechanism of Ethylene Epoxidation Catalysis. *Catal. Lett.* **2013**, *143* (2), 131–141.
- (5) Galvanin, F.; Cao, E.; Al-Rifai, N.; Dua, V.; Gavriilidis, A. Optimal Design of Experiments for the Identification of Kinetic Models of Methanol Oxidation over Silver Catalyst. *Chem. Today* **2015**, *33*, 51.
- (6) Besenbacher, F.; Nørskov, J. K. Oxygen Chemisorption on Metal Surfaces: General Trends for Cu, Ni and Ag. *Prog. Surf. Sci.* **1993**, *44* (1), 5–66.
- (7) Campbell, C. T. Chlorine Promoters in Selective Ethylene Epoxidation over Ag(111): A Comparison with Ag(110). *J. Catal.* **1986**, *99* (1), 28–38.
- (8) Cant, N. W.; Hall, W. K. Catalytic Oxidation. VI. Oxidation of Labeled Olefins over Silver. *J. Catal.* **1978**, *52* (1), 81–94.
- (9) Linic, S.; Barteau, M. A. Control of Ethylene Epoxidation Selectivity by Surface Oxametallacycles. *J. Am. Chem. Soc.* **2003**, *125* (14), 4034–4035.
- (10) Jankowiak, J. T.; Barteau, M. A. Ethylene Epoxidation over Silver and Copper-Silver Bimetallic Catalysts: II. Cs and Cl Promotion. *J. Catal.* **2005**, *236* (2), 379–386.
- (11) Grant, R. B.; Lambert, R. M. A Single Crystal Study of the Silver-Catalysed Selective Oxidation and Total Oxidation of Ethylene. *J. Catal.* **1985**, *92* (2), 364–375.

(12) Nguyen, N. L.; De Gironcoli, S.; Piccinin, S. Ag-Cu Catalysts for Ethylene Epoxidation: Selectivity and Activity Descriptors. *J. Chem. Phys.* **2013**, *138* (18), 184707.

(13) Nguyen, N. L.; Piccinin, S.; De Gironcoli, S. Stability of Intermediate States for Ethylene Epoxidation on Ag-Cu Alloy Catalyst: A First-Principles Investigation. *J. Phys. Chem. C* **2011**, *115* (20), 10073–10079.

(14) Bendounan, A.; Forster, F.; Ziroff, J.; Schmitt, F.; Reinert, F. Influence of the Reconstruction in AgCu(111) on the Surface Electronic Structure: Quantitative Analysis of the Induced Band Gap. *Phys. Rev. B: Condens. Matter Mater. Phys.* **2005**, *72* (7), No. 075407.

(15) Greeley, J.; Mavrikakis, M. Near-Surface Alloys for Hydrogen Fuel Cell Applications. *Catal. Today* **2006**, *111* (1–2), 52–58.

(16) Stamenkovic, V. R.; Mun, B. S.; Arenz, M.; Mayrhofer, K. J. J.; Lucas, C. A.; Wang, G.; Ross, P. N.; Markovic, N. M. Trends in Electrocatalysis on Extended and Nanoscale Pt-Bimetallic Alloy Surfaces. *Nat. Mater.* **2007**, *6* (3), 241–247.

(17) Zhang, J.; Vukmirovic, M. B.; Sasaki, K.; Nilekar, A. U.; Mavrikakis, M.; Adzic, R. R. Mixed-Metal Pt Monolayer Electrocatalysts for Enhanced Oxygen Reduction Kinetics. *J. Am. Chem. Soc.* **2005**, *127* (36), 12480–12481.

(18) Zhao, Z.; Lu, G. Computational Screening of Near-Surface Alloys for CO₂ Electroreduction. *ACS Catal.* **2018**, *8* (5), 3885–3894.

(19) Besenbacher, F.; Chorkendorff, I.; Clausen, B. S.; Hammer, B.; Molenbroek, A. M.; Nørskov, J. K.; Stensgaard, I. Design of a Surface Alloy Catalyst for Steam Reforming. *Science (Washington, DC, U. S.)* **1998**, *279* (5358), 1913–1915.

(20) Knudsen, J.; Nilekar, A. U.; Vang, R. T.; Schnadt, J.; Kunkes, E. L.; Dumesic, J. A.; Mavrikakis, M.; Besenbacher, F. A Cu/Pt near-Surface Alloy for Water-Gas Shift Catalysis. *J. Am. Chem. Soc.* **2007**, *129* (20), 6485–6490.

(21) Greeley, J.; Mavrikakis, M. Alloy Catalysts Designed from First Principles. *Nat. Mater.* **2004**, *3* (11), 810–815.

(22) Bendounan, A.; Cercellier, H.; Fagot-Revurat, Y.; Kierren, B.; Yurov, V. Y.; Malterre, D. Modification of Shockley States Induced by Surface Reconstruction in Epitaxial Ag Films on Cu(111). *Phys. Rev. B: Condens. Matter Mater. Phys.* **2003**, *67* (16), 165412.

(23) McMahon, W. E.; Hirschorn, E. S.; Chiang, T. C. Scanning Tunneling Microscopy Study of a Ag Monolayer on Cu(111). *Surf. Sci.* **1992**, *279* (3), L231–L235.

(24) Meunier, I.; Treglia, G.; Gay, J.-M.; Aufray, B.; Legrand, B. Ag/Cu(111) Structure Revisited through an Extended Mechanism for Stress Relaxation. *Phys. Rev. B: Condens. Matter Mater. Phys.* **1999**, *59* (16), 10910–10917.

(25) Umezawa, K.; Nakanishi, S.; Yoshimura, M.; Ojima, K.; Ueda, K.; Gibson, W. M. Ag/Cu(111) Surface Structure and Metal Epitaxy by Impact-Collision Ion-Scattering Spectroscopy and Scanning Tunneling Microscopy. *Phys. Rev. B: Condens. Matter Mater. Phys.* **2000**, *63* (3), 035402.

(26) Campbell, C. T. Atomic and Molecular Oxygen Adsorption on Ag(111). *Surf. Sci.* **1985**, *157* (1), 43–60.

(27) Bellisario, D. O.; Han, J. W.; Tierney, H. L.; Baber, A. E.; Sholl, D. S.; Sykes, E. C. H. Importance of Kinetics in Surface Alloying: A Comparison of the Diffusion Pathways of Pd and Ag Atoms on Cu(111). *J. Phys. Chem. C* **2009**, *113* (29), 12863–12869.

(28) Johnston, S. M.; Mulligan, A.; Dhanak, V.; Kadodwala, M. The Structure of Disordered Chemisorbed Oxygen on Cu(1 1 1). *Surf. Sci.* **2002**, *519* (1–2), 57–63.

(29) Hashizume, T.; Taniguchi, M.; Motai, K.; Lu, H.; Tanaka, K.; Sakurai, T. Scanning Tunneling Microscopy of Oxygen Adsorption on the Ag(110) Surface. *Surf. Sci.* **1992**, *266* (1–3), 282–284.

(30) Carlisle, C. I.; Fujimoto, T.; Sim, W. S.; King, D. A. Atomic Imaging of the Transition between Oxygen Chemisorption and Oxide Film Growth on Ag{111}. *Surf. Sci.* **2000**, *470* (1–2), 15–31.

(31) de Mongeot, F. B.; Valbusa, U.; Rocca, M. Oxygen Adsorption on Ag(111). *Surf. Sci.* **1995**, *339* (3), 291–296.

(32) Campbell, C. T. Cs-Promoted Ag(111): Model Studies of Selective Ethylene Oxidation Catalysts. *J. Phys. Chem.* **1985**, *89* (26), 5789–5795.

(33) Raukema, A.; Butler, D. A.; Box, F. M. A.; Kleyn, A. W. Dissociative and Non-Dissociative Sticking of O₂ at the Ag(111) Surface. *Surf. Sci.* **1996**, *347* (1–2), 151–168.

(34) Steininger, H.; Lehwald, S.; Ibach, H. Adsorption of Oxygen on Pt(111). *Surf. Sci.* **1982**, *123* (1), 1–17.

(35) Zambelli, T.; Barth, J. V.; Wintterlin, J.; Ertl, G. Complex Pathways in Dissociative Adsorption of Oxygen on Platinum. *Nature* **1997**, *390* (6659), 495–497.

(36) Min, B. K.; Alemozafar, A. R.; Biener, M. M.; Biener, J.; Friend, C. M. Reaction of Au(111) with Sulfur and Oxygen: Scanning Tunneling Microscopic Study. *Top. Catal.* **2005**, *36* (1–4), 77–90.

(37) Deng, X.; Min, B. K.; Guloy, A.; Friend, C. M. Enhancement of O₂ Dissociation on Au(111) by Adsorbed Oxygen: Implications for Oxidation Catalysis. *J. Am. Chem. Soc.* **2005**, *127* (25), 9267–9270.

(38) Vattuone, L.; Yeo, Y. Y.; King, D. A. Adatom Bond Energies and Lateral Interaction Energies from Calorimetry: NO, O₂, and N₂ Adsorption on Ni{100}. *J. Chem. Phys.* **1996**, *104* (20), 8096–8102.

(39) Tyson, W. R.; Miller, W. A. Surface Free Energies of Solid Metals: Estimation from Liquid Surface Tension Measurements. *Surf. Sci.* **1977**, *62* (1), 267–276.

(40) Hirsimäki, M.; Lampimäki, M.; Lahtonen, K.; Chorkendorff, I.; Valden, M. Investigation of the Role of Oxygen Induced Segregation of Cu during Cu₂O Formation on Cu{1 0 0}, Ag/Cu{1 0 0} and Cu(Ag) Alloy. *Surf. Sci.* **2005**, *583* (2–3), 157–165.

(41) Piccinin, S.; Stampfli, C.; Scheffler, M. Ag-Cu Alloy Surfaces in an Oxidizing Environment: A First-Principles Study. *Surf. Sci.* **2009**, *603* (10–12), 1467–1475.

(42) Towns, J.; Cockerill, T.; Dahan, M.; Foster, I.; Gaither, K.; Grimshaw, A.; Hazlewood, V.; Lathrop, S.; Lifka, D.; Peterson, G. D.; Roskies, R.; Scott, J. R.; Wilkins-Diehr, N. XSEDE: Accelerating Scientific Discovery. *Comput. Sci. Eng.* **2014**, *16*, 62–74.